NASA TECHNICAL NOTE

NASA TN D-2606

C.1

LOAN COPY: RET
AFWL (WLIL
KIRTLAND AFB,

0079626

TECH LIBRARY KAFB, NM

NASA TN D-2606

AERODYNAMIC CHARACTERISTICS OF LENTICULAR AND ELLIPTIC SHAPED CONFIGURATIONS AT A MACH NUMBER OF 6

by J. Wayne Keyes

Langley Research Center
Langley Station, Hampton, Va.

NATIONAL AERONAUTICS AND SPACE ADMINISTRATION • WASHINGTON, D. C. • FEBRUARY 1965

TECH LIBRARY KAFB, NM

0079626

AERODYNAMIC CHARACTERISTICS OF LENTICULAR AND ELLIPTIC SHAPED CONFIGURATIONS AT A MACH NUMBER OF 6

By J. Wayne Keyes

Langley Research Center
Langley Station, Hampton, Va.

NATIONAL AERONAUTICS AND SPACE ADMINISTRATION

For sale by the Office of Technical Services, Department of Commerce,
Washington, D.C. 20230 -- Price $2.00

AERODYNAMIC CHARACTERISTICS OF LENTICULAR AND ELLIPTIC SHAPED CONFIGURATIONS AT A MACH NUMBER OF 6

By J. Wayne Keyes
Langley Research Center

SUMMARY

Force and moment data were obtained for two groups of lifting reentry configurations. One group consisted of five elliptic-lenticular configurations and the other group consisted of five three-dimensional ellipsoid configurations. The thickness-chord ratio varied from 0.3 to 0.9 for both groups.

The results of the investigation indicate that in general all of the configurations were statically unstable at angles of attack near 0° with the center of gravity at 50 percent of the maximum chord. A forward movement of the center of gravity to 40-percent chord results in a stable condition at 0° for thickness-chord ratios greater than about 0.72 for the elliptic-lenticular configurations and about 0.77 for the three-dimensional ellipsoid configurations. All of the configurations are stable near 90° angle of attack for both center-of-gravity locations. However, the configurations are less stable with increasing thickness-chord ratio.

In general, the three-dimensional ellipsoid configurations have a higher maximum lift coefficient for either a given maximum lift-drag ratio or for a given thickness ratio. From the standpoint of useful volume, the elliptic-lenticular configurations are slightly more efficient in that they have a higher maximum lift-drag ratio for a given volume.

In general, values obtained by use of modified Newtonian theory give a good indication of the trend of the experimental data for the elliptic-lenticular configurations.

INTRODUCTION

Among the investigations being made by the National Aeronautics and Space Administration are studies of spacecraft configurations that have the capability of reentering the earth's atmosphere at near-escape speed and of maneuvering and landing at preselected sites. Such a vehicle would probably enter the atmosphere at a high angle of attack (near 90°) in order to utilize maximum drag. A decrease in angle of attack would then generate lift or side forces to control the trajectory. After the vehicle has passed through the critical phases of reentry (high speed, high deceleration, and heating), the angle of attack would be decreased further to allow the vehicle to glide to a landing. (See ref. 1.)

A configuration which might satisfy these conditions is a lenticular or ellipsoid shaped body. Since this type of vehicle could have both a low ratio of weight to drag and a large radius of curvature of the exposed surface at high angles of attack, a low total heat input would be anticipated. The lift-drag ratio at low angles of attack would most likely be sufficient for landing purposes. (See ref. 2.)

This investigation was initiated to obtain the effects of thickness-chord ratio and body shape on the aerodynamic characteristics of two groups of basic (no controls) lifting reentry configurations. The models had elliptic cross sections with the thickness-chord ratio varying from 0.3 to 0.9. One group had a circular planform and the other group had an elliptic planform. The investigation was conducted at a Mach number of 6. Studies of similar shapes have been conducted at subsonic, transonic, and supersonic Mach numbers and the results have been reported in references 2 to 11.

SYMBOLS

b	span of model, in.
C_A	body axial-force coefficient, $F_A/q_\infty S$
C_D	drag coefficient, $D/q_\infty S$
C_L	lift coefficient, $L/q_\infty S$
C_{L_α}	lift-curve slope, $\partial C_L/\partial\alpha$
C_m	pitching-moment coefficient, $M_Y/q_\infty Sc$
C_{m_α}	pitching-moment-curve slope, $\partial C_m/\partial\alpha$
C_N	body normal-force coefficient, $F_N/q_\infty S$
c	maximum chord of model, in.
c.g.	center of gravity and moment reference center
D	drag, lb
F_A	axial force, lb

F_N	normal force, lb
L	lift, lb
L/D	lift-drag ratio
M_Y	pitching moment, in-lb
q_∞	free-stream dynamic pressure, lb/sq in. abs
S	planform area of model, sq in.
t	maximum thickness of model, in.
t/c	thickness-chord ratio (see fig. 2)
V	volume of model, cu in.
α	angle of attack of model center line, deg
α_1	angle between model center line and sting center line, deg

Subscripts:

max	maximum
min	minimum

APPARATUS, TESTS, AND MODELS

Tunnel

The investigation was conducted in the Langley 20-inch Mach 6 tunnel, which is of the intermittent or blowdown type, exhausting into the atmosphere. The tunnel can operate at stagnation pressures from about 7 to 37 atmospheres and stagnation temperatures up to 600° F. A more complete description of the tunnel is given in reference 12.

Sting and Support System

The tunnel has a gooseneck-type strut support system which operates in the horizontal plane with a strut-support angle-of-attack range from about -15° to 30°. As a means of covering the complete model angle-of-attack range with minimum sting effects, two stings (straight sting and 30° bent sting) were used in conjunction with two model mounting positions as shown in figure 1. Model and sting positions are given in the following table:

Angle-of-attack range, deg	Sting angle, deg	Model position α_1, deg
-5 to 30	0	0
25 to 60	30 (bent)	0
60 to 95	0	90

Tests

The tests were conducted at a Mach number of 6 with a stagnation pressure of about 27.7 atmospheres and a free-stream Reynolds number of 7.96×10^6 per foot. Tunnel stagnation temperature was maintained at about 400° F, a temperature sufficient to prevent liquefaction of the air. The model angle of attack varied from -5° to 95°.

Models

The models were divided into two groups; one group consisted of five models which had lenticular shapes (elliptic cross section and circular planform), and the second group consisted of five models which were three-dimensional ellipsoids (elliptic cross sections in all three axis planes). The thickness ratio t/c was varied from 0.3 to 0.9 for both groups. The planform area for all models was held constant at 24 square inches. The geometric characteristics of both groups of models and the model code system used are presented in figure 2. Photographs of the models are shown in figure 3.

MEASUREMENTS AND ACCURACY

Aerodynamic forces and moments were measured with a six-component strain-gage balance, which was located either internally or externally, depending on the model. The balance was shielded from the air flow at all times. The force and moment coefficients are referred to the body-axis system shown in figure 1; however, all data are presented about the stability axis system. For all models, the pitching-moment data are presented about each of two positions (40 and 50 percent of the maximum chord from the forward edge of the model). The axial-force coefficient has not been corrected for base pressure effects.

Estimates of accuracy were made on the basis of calibrations and repeatability of data. Measured quantities are considered accurate within the following limits:

C_A . . . . ±0.014
C_D . . . . ±0.013
C_L . . . . ±0.013

C_m . . . . ± 0.009
C_N . . . . ± 0.011

The accuracy of angle of attack and of free-stream Mach number is estimated to be within $\pm 0.1^\circ$ and ± 0.02, respectively.

RESULTS AND DISCUSSION

The basic aerodynamic characteristics plotted against angle of attack are presented in figure 4 for the elliptic-lenticular configurations and in figure 5 for the three-dimensional ellipsoid configurations. All of the configurations except the ellipsoid model with thickness-chord ratio of 0.3 were tested at angles of attack from -5° to 95° (fig. 5(a)). No data were obtained for this configuration from 10° to 30° because of tunnel-wall interference. Figures 6, 7, and 8 are summary plots of the slopes and selected aerodynamic characteristics at low angles of attack (near $\alpha = 0^\circ$), at $\alpha = 90^\circ$, and at maximum lift-drag ratio for various thickness ratios. The slopes in figure 6 were taken at α between -5° and 5° and in figure 7 at α between 85° and 95°. Composite plots of the lift coefficient at maximum lift-drag ratio and the maximum lift coefficient are presented in figure 9. The variations of both the maximum lift-drag ratio with a volumetric efficiency parameter and the lift coefficient at maximum lift-drag ratio with the same parameter are shown in figure 10. The volumetric efficiency parameter is based on the total volume to the 2/3 power (ref. 13) and the planform area, which remains the same for all configurations.

Theoretical estimates of the variation of the aerodynamic characteristics with angle of attack are presented for comparison with the measured data in figure 4 for the elliptic-lenticular configurations. Slopes obtained from these theoretical curves are plotted in figures 6, 7, and 8 for comparison with the measured slopes. Modified Newtonian theory based on the method of reference 14 was used to calculate these estimates. The stagnation pressure behind a normal shock was used in this method to obtain the maximum value of the pressure coefficient. In general, values obtained by use of modified Newtonian theory give a good indication of the trend of the experimental data for the elliptic-lenticular configurations.

All configurations had a stable trim point at angles of attack between 80° and 90° with the center of gravity located at 0.5c. When the center of gravity was moved forward to the 0.4c position for the elliptic-lenticular configurations, the trim angle of attack was decreased. For the 0.3-thickness ratio, the trim angle of attack was 42° and as the thickness ratio was increased from 0.3 to 0.9, the trim angle of attack increased to 50° and then decreased to about 0°. A similar trend was noted for the three-dimensional ellipsoid configuration, except that the initial increase in trim angle of attack with increasing thickness ratio was from 32° to 40°. (See figs. 4 and 5.)

As expected, all configurations were unstable near $\alpha = 0^\circ$ for the most rearward center-of-gravity location (0.5c). However, a forward movement of the center of gravity to 0.4c resulted in a stable condition near $\alpha = 0^{\circ}$ for thickness ratios greater than about 0.72 for the elliptic-lenticular configurations and about 0.77 for the three-dimensional ellipsoid configurations. (See fig. 6.) The moment characteristics for $\alpha = 90^{\circ}$ indicate that all configurations are stable for both center-of-gravity locations and that the configurations are less stable with increasing thickness ratio (fig. 7).

The drag coefficient at $\alpha = 90^{\circ}$ is decreasing with increasing thickness ratio rather than increasing as at $\alpha = 0^{\circ}$, since the amount of bluntness in the free-stream direction is decreasing. This trend was observed for both the elliptic-lenticular configurations and the three-dimensional ellipsoid configurations.

The longitudinal aerodynamic parameters at maximum lift-drag ratio (fig. 8) show that the pitching moment and lift-curve slopes follow the same trends for both groups of configurations, that is, a decrease with increasing thickness ratio. The angle of attack at which maximum lift-drag ratio occurs is approximately the same for a given thickness ratio in each group.

A comparison of the lift characteristics of both the elliptic-lenticular and the three-dimensional ellipsoid configurations indicates that the ellipsoid configurations have a higher maximum lift coefficient for either a given maximum lift-drag ratio or for a given thickness ratio (fig. 9). As expected, the maximum lift-drag ratio decreases with increasing thickness ratio. The magnitude of the maximum lift-drag ratios for the ellipsoid configurations are higher than those for the lenticular configurations for the same thickness ratio (fig. 9). From the standpoint of useful volume, however, the elliptic-lenticular configurations are slightly more efficient in that they have a higher maximum lift-drag ratio for a given volume (fig. 10). The lenticular configurations also have slightly more lift at maximum lift-drag ratio than the ellipsoid configuration for a given volume.

CONCLUSIONS

The results of an investigation of two groups of lifting reentry configurations with lenticular and elliptic shapes and various thickness ratios indicate the following conclusions:

1. In general, all configurations were statically unstable at angles of attack near 0° with the center of gravity at 50 percent of the maximum chord. A forward movement of the center of gravity to 40-percent chord results in a stable condition at 0° for thickness-chord ratios greater than about 0.72 for the elliptic-lenticular configurations and about 0.77 for the three-dimensional ellipsoid configurations.

2. All configurations are stable near an angle of attack of 90° for both center-of-gravity locations. However, the configurations are less stable with increasing thickness-chord ratio.

3. The three-dimensional ellipsoid configurations have a higher maximum lift coefficient for either a given maximum lift-drag ratio or for a given thickness ratio.

4. From the standpoint of useful volume, the elliptic-lenticular configurations are slightly more efficient in that they have a higher maximum lift-drag ratio for a given volume.

5. In general, values obtained by use of modified Newtonian theory give a good indication of the trend of the experimental data for the elliptic-lenticular configurations.

Langley Research Center,
National Aeronautics and Space Administration,
Langley Station, Hampton, Va., October 15, 1964.

REFERENCES

1. Staff of Langley Flight Research Division (Donald C. Cheatham, compiler): A Concept of a Manned Satellite Reentry Which Is Completed With a Glide Landing. NASA TM X-226, 1959.

2. Demele, Fred A.; and Brownson, Jack J.: Subsonic Longitudinal Aerodynamic Characteristics of Disks With Elliptic Cross Sections and Thickness-Diameter Ratios From 0.225 to 0.425. NASA TN D-788, 1961.

3. Demele, Fred A.; and Brownson, Jack J.: Subsonic Aerodynamic Characteristics of Disk Re-Entry Configurations With Elliptic Cross Sections and Thickness-Diameter Ratios of 0.225 and 0.325. NASA TM X-566, 1961.

4. Mugler, John P., Jr.; and Olstad, Walter B.: Static Longitudinal Aerodynamic Characteristics at Transonic Speeds of a Lenticular-Shaped Reentry Vehicle. NASA TM X-423, 1960.

5. Lazzeroni, Frank A.: Experimental Investigation of a Disk-Shaped Reentry Configuration at Transonic and Low Supersonic Speeds. NASA TM X-652, 1962.

6. Jackson, Charlie M., Jr.; and Harris, Roy V., Jr.: Static Longitudinal Stability and Control Characteristics at a Mach Number of 1.99 of a Lenticular-Shaped Reentry Vehicle. NASA TN D-514, 1960.

7. Lazzeroni, Frank A.: Aerodynamic Characteristics of Two Disk Re-Entry Configurations at a Mach Number of 2.2. NASA TM X-567, 1961.

8. Letko, William: Experimental Investigation at a Mach Number of 3.11 of the Lift, Drag, and Pitching-Moment Characteristics of Five Blunt Lifting Bodies. NASA TN D-226, 1960.

9. McShera, John T., Jr.; and Lowery, Jerry L.: Static Stability and Longitudinal Control Characteristics of a Lenticular-Shaped Reentry Vehicle at Mach Numbers of 3.5 and 4.65. NASA TM X-763, 1963.

10. Olstad, Walter B.; and Wornom, Dewey E.: Static Longitudinal Stability and Control Characteristics at Mach Numbers of 2.86 and 6.02 and Angles of Attack up to 95° of a Lenticular-Shaped Reentry Vehicle. NASA TM X-621, 1961.

11. Rainey, Robert W., compiler: Summary of Aerodynamic Characteristics of Low-Lift-Drag-Ratio Reentry Vehicles From Subsonic to Hypersonic Speeds. NASA TM X-588, 1961.

12. Sterrett, James R.; and Emery, James C.: Extension of Boundary-Layer-Separation Criteria to a Mach Number of 6.5 by Utilizing Flat Plates With Forward-Facing Steps. NASA TN D-618, 1960.

13. Bertram, Mitchel H.; Fetterman, David E., Jr.; and Henry, John R.: The Aerodynamics of Hypersonic Cruising and Boost Vehicles. Proceedings of the NASA-University Conference on the Science and Technology of Space Exploration, Vol. 2, NASA SP-11, 1962, pp. 215-234. (Also available as NASA SP-23.)

14. Keyes, J. Wayne: Longitudinal Aerodynamic Characteristics of Blunted Cones at Mach Numbers of 3.5, 4.2, and 6.0. NASA TN D-2201, 1964.

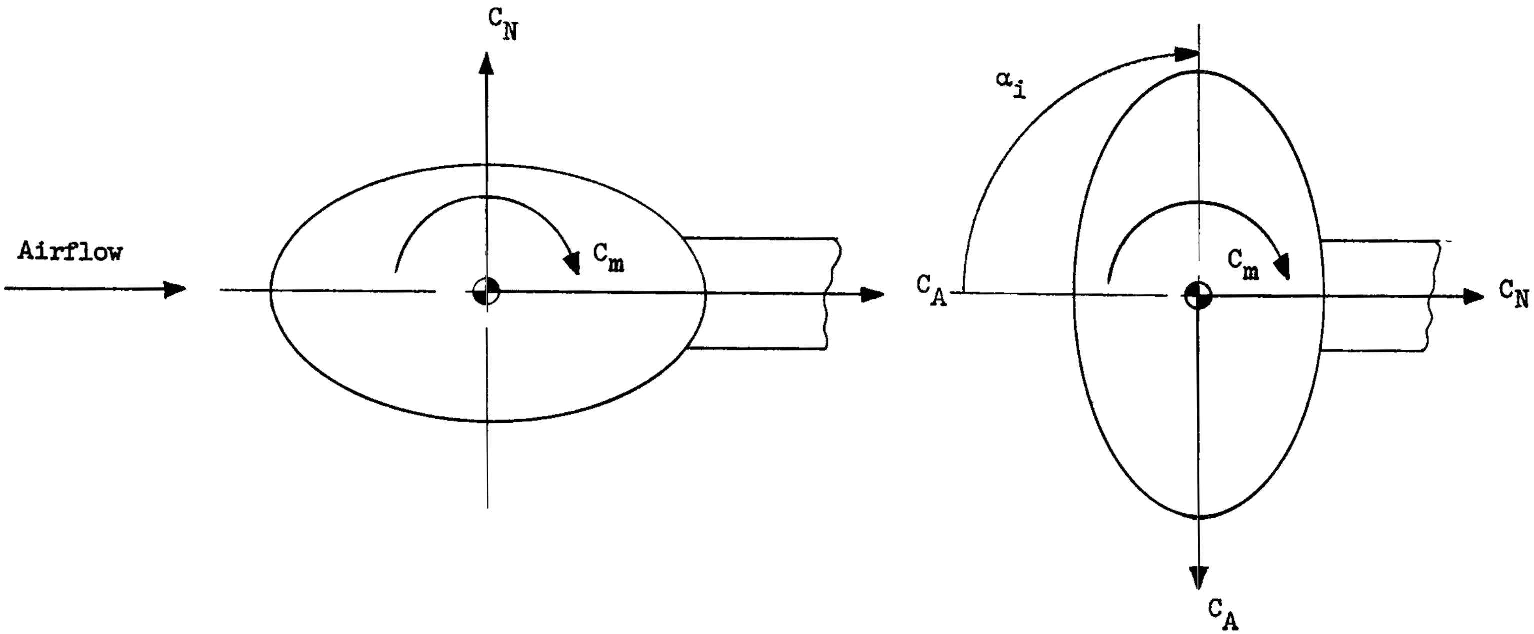

$\alpha_i = 0^{\circ}$ $\alpha_i = 90^{\circ}$

Figure 1.- Model mounting positions and body-axis system. (Arrows indicate positive directions.)

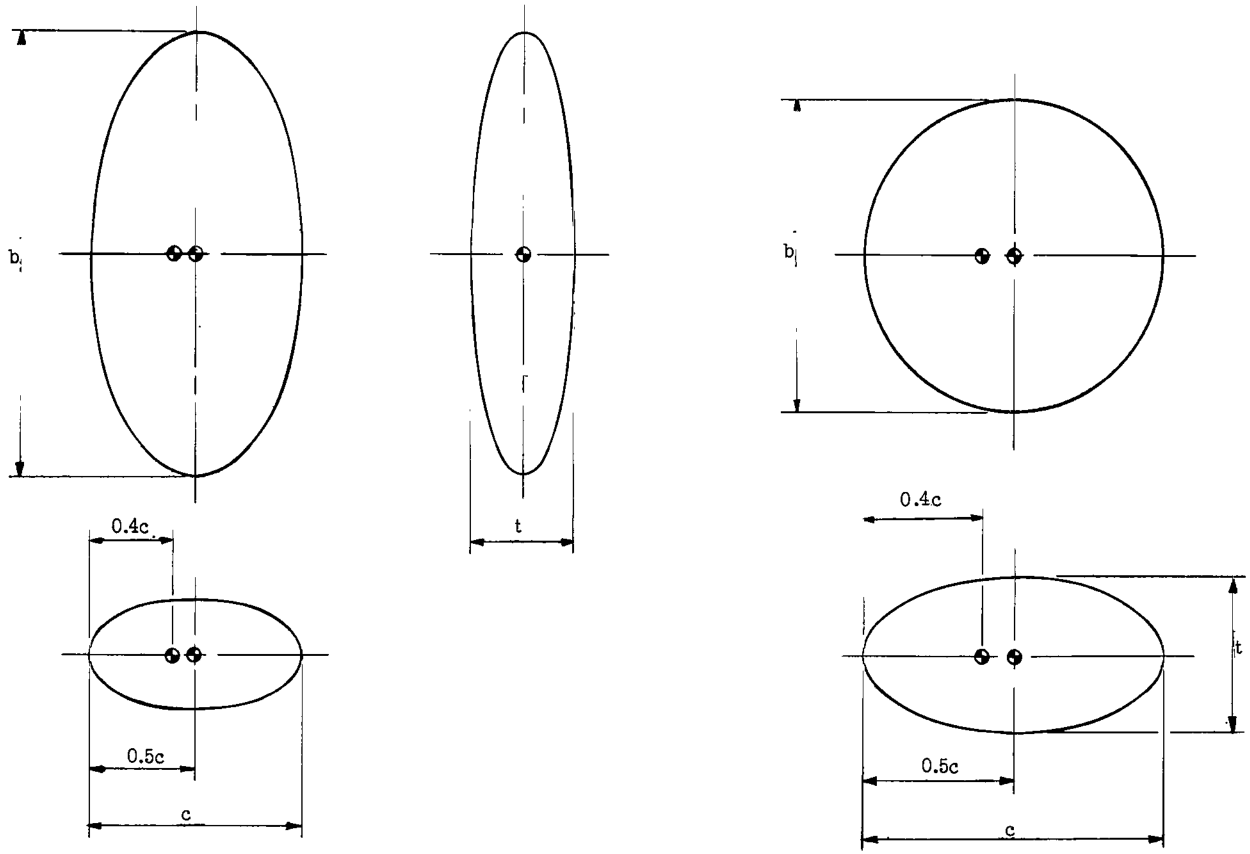

Model	t/c	b	c	t
L-E0	0.3	10.092	3.028	0.908
L-E1	.5	7.818	3.908	1.954
L-E2	.6	7.136	4.282	2.569
L-E3	.7	6.608	4.624	3.237
L-E4	.9	5.828	5.244	4.720

(a) Three-dimensional ellipsoid models; $t/c = c/b$; $(t/c)^2 = t/b$.

Model	t/c	c	t
L-L0	0.3	5.528	1.658
L-L1	.5	5.528	2.764
L-L2	.6	5.528	3.317
L-L3	.7	5.528	3.870
L-L4	.9	5.528	4.975

(b) Elliptic-lenticular models; $c/b = 1$.

Figure 2.- Geometric characteristics of models. (All dimensions are in inches unless otherwise noted.)

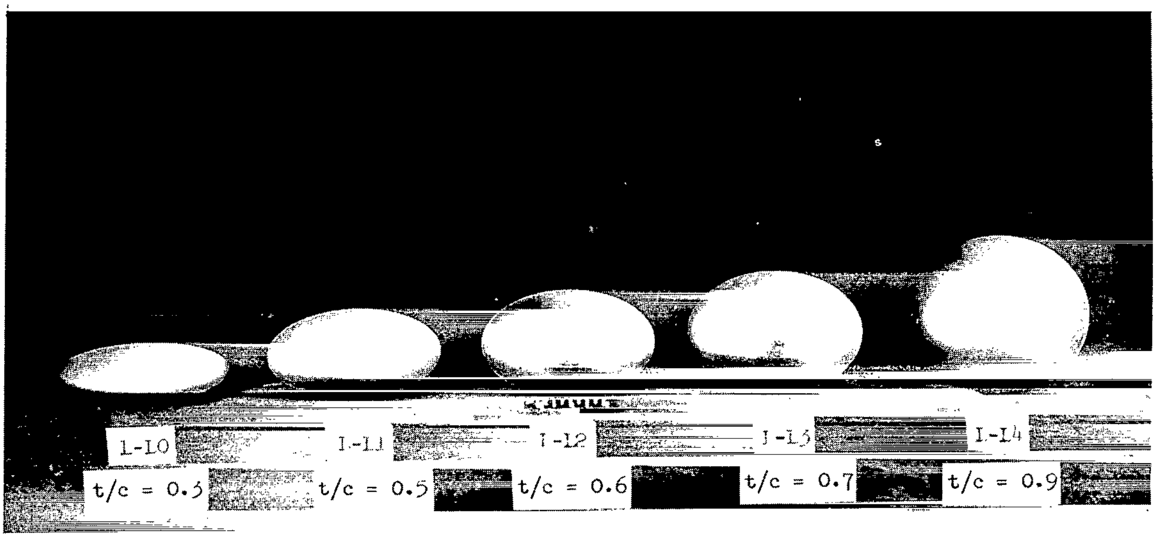

(a) Elliptic-lenticular models. L-61-1228.1

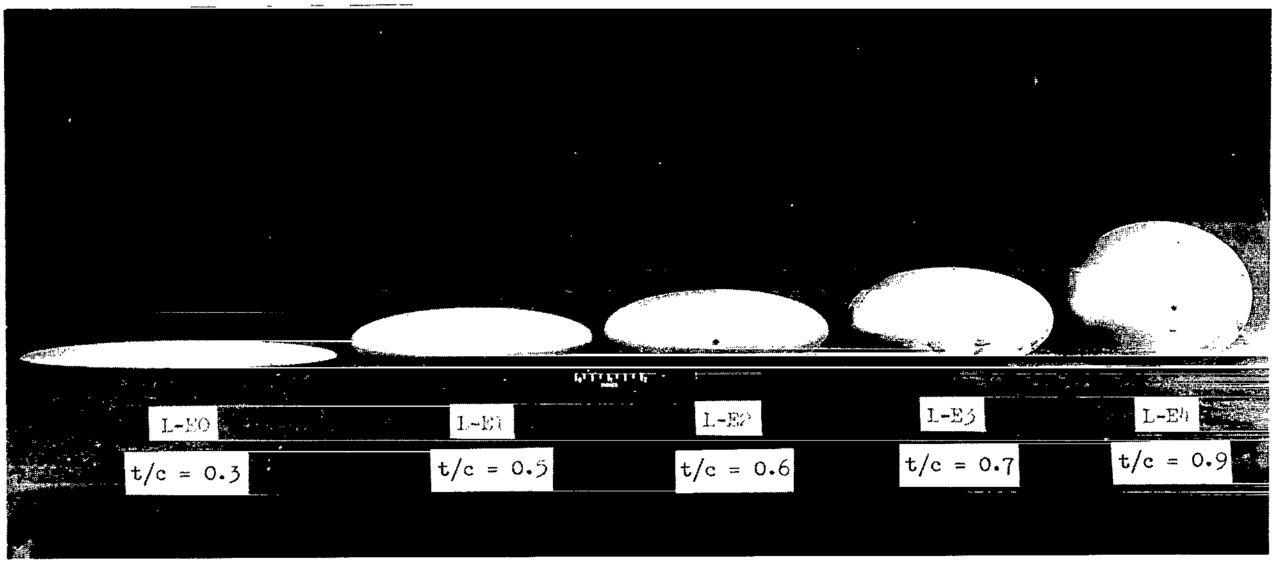

(b) Three-dimensional ellipsoid models. L-61-1229.1

Figure 3.- Photographs of model.

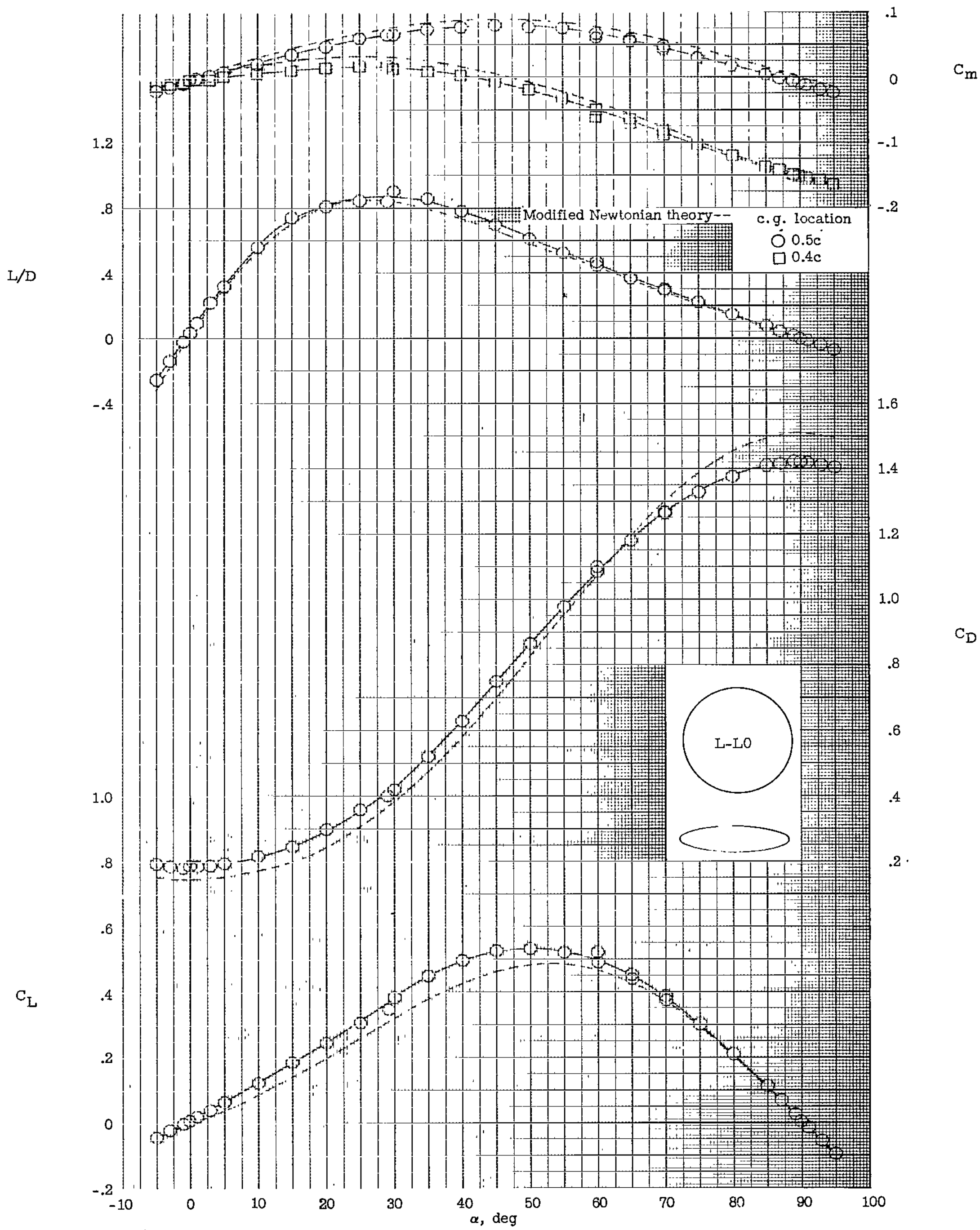

(a) L-LO (t/c = 0.3).

Figure 4.- Aerodynamic characteristics of elliptic-lenticular models.

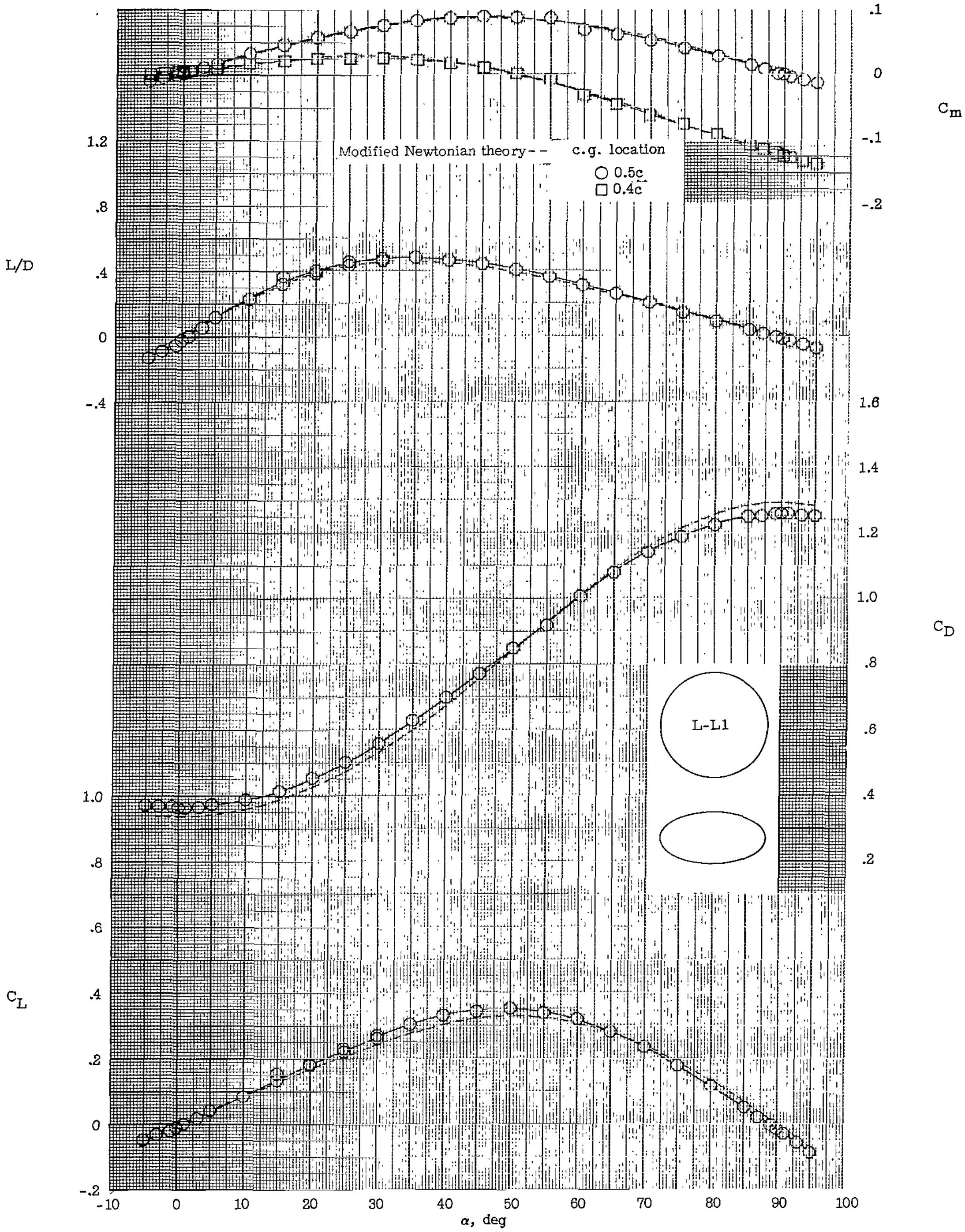

(b) L-L1 (t/c = 0.5).

Figure 4.- Continued.

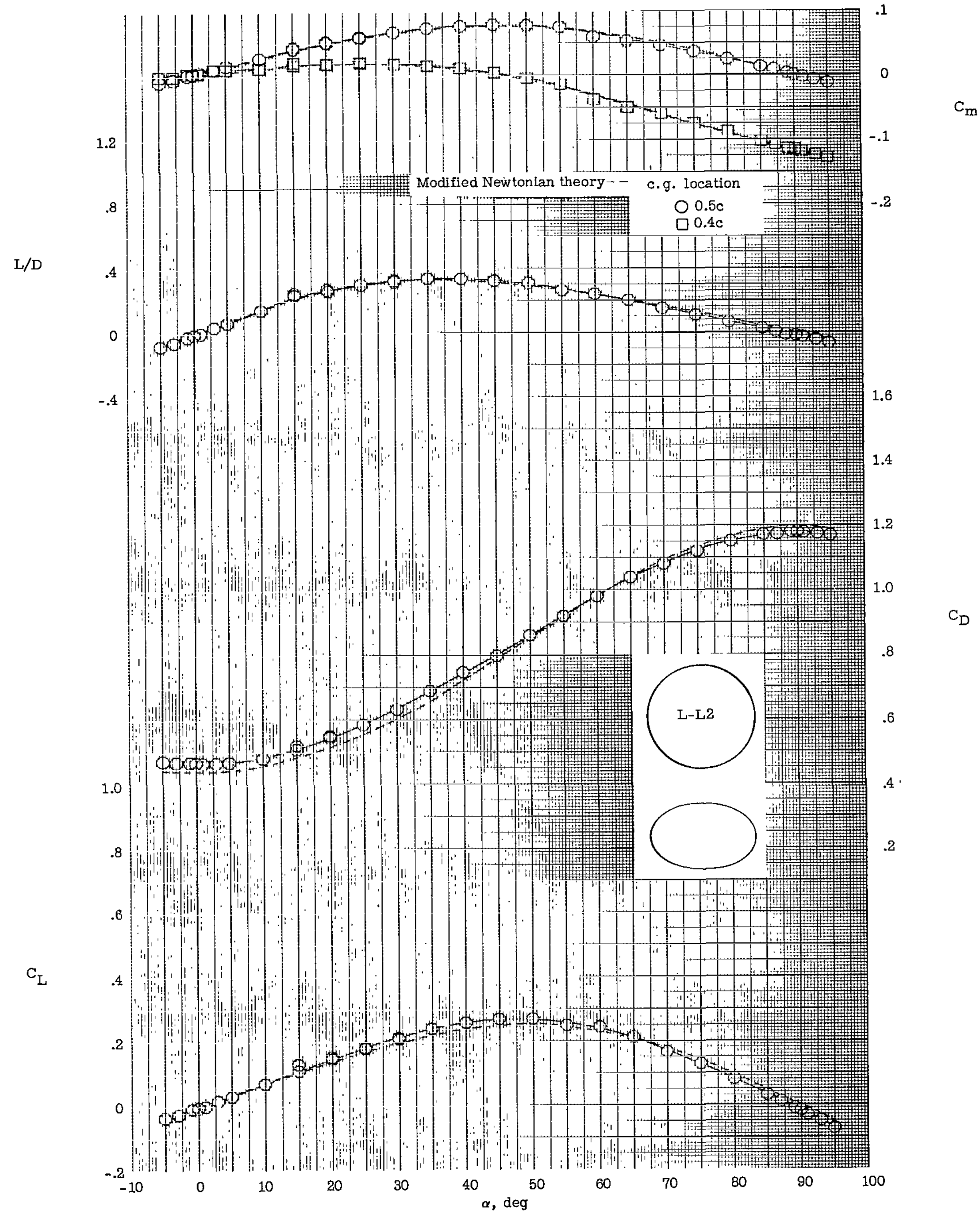

(c) L-L2 (t/c = 0.6).

Figure 4.- Continued.

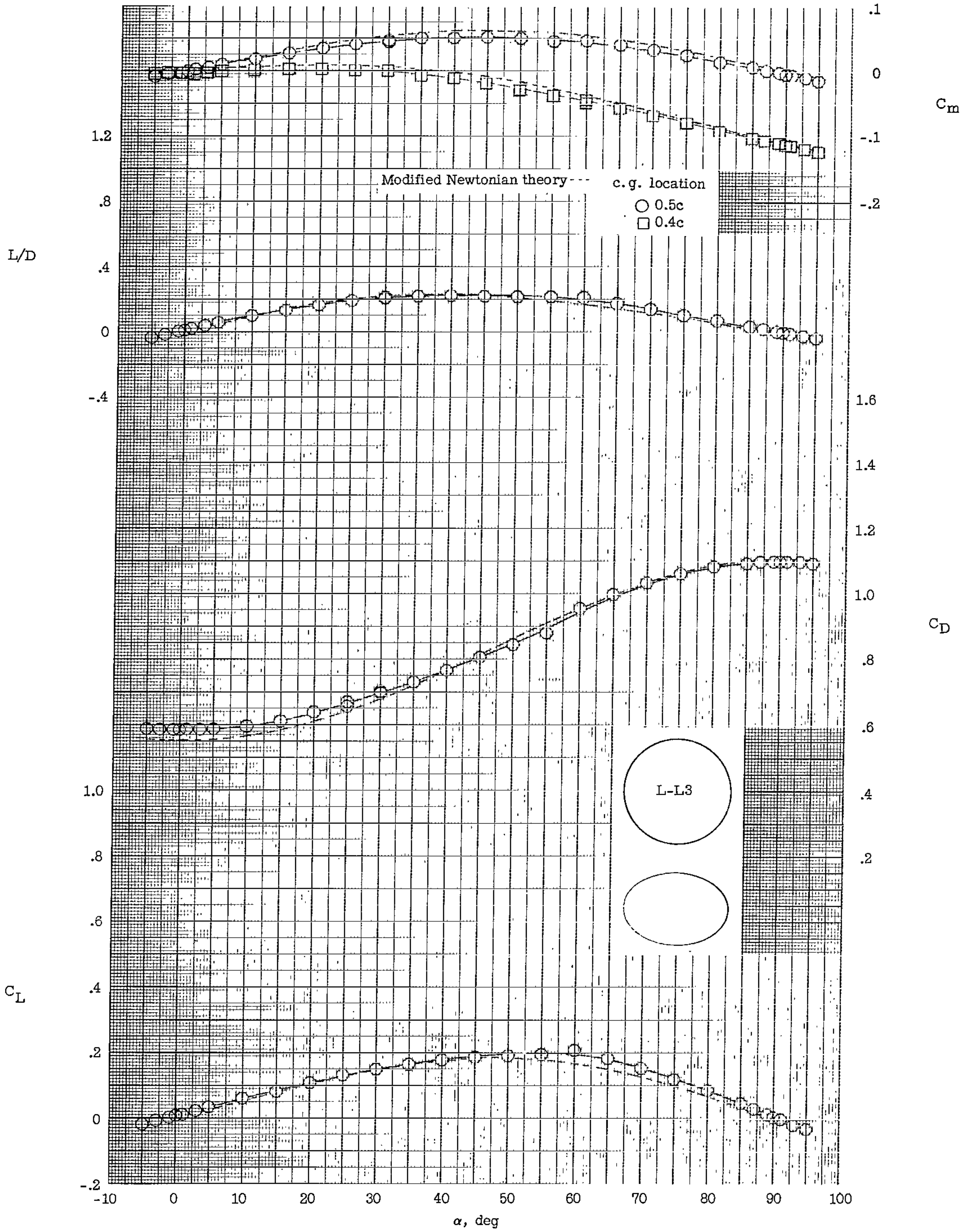

(d) L-L3 (t/c = 0.7).

Figure 4.- Continued.

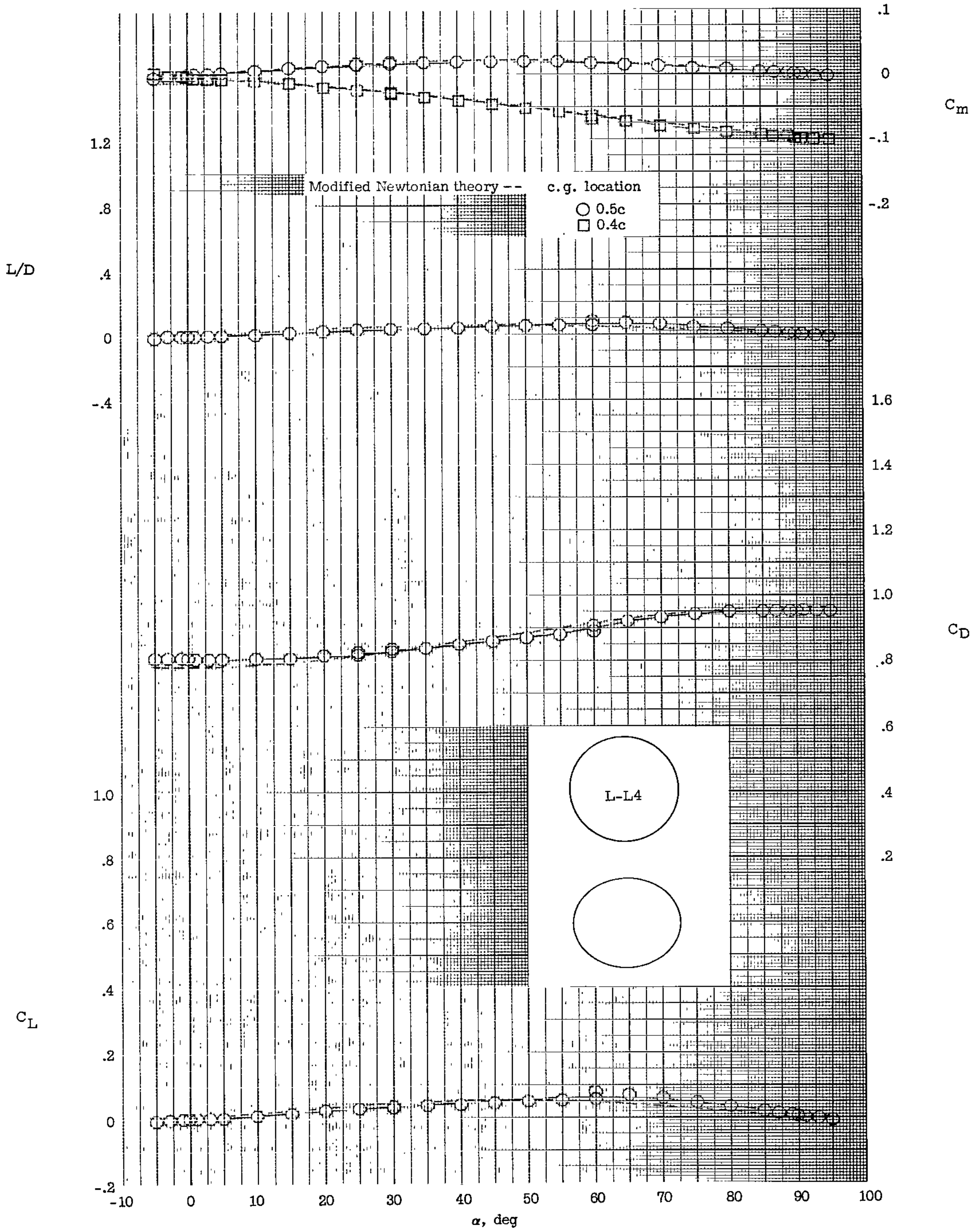

(e) L-L4 (t/c = 0.9).

Figure 4.- Concluded.

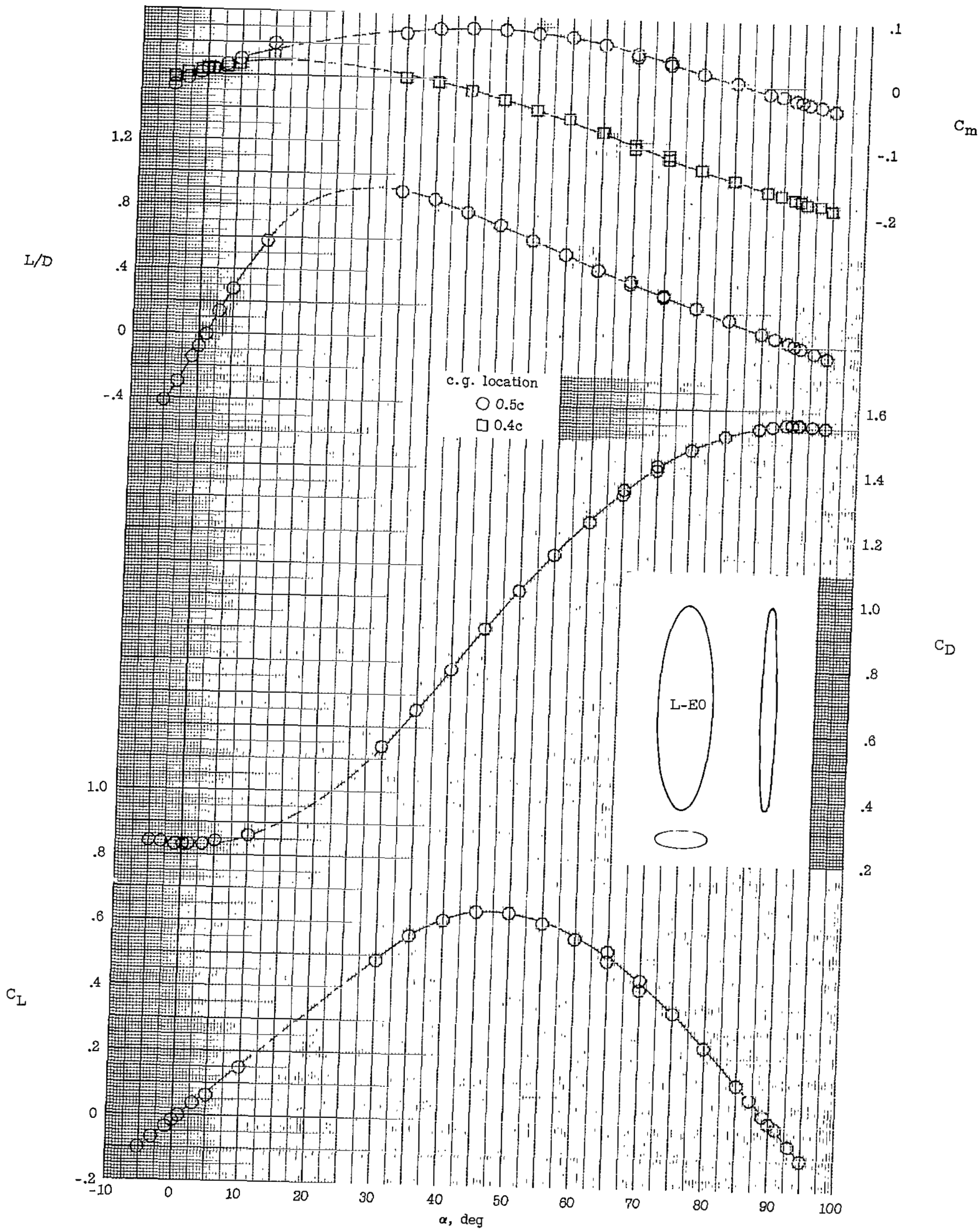

(a) L-EO (t/c = 0.3).

Figure 5.- Aerodynamic characteristics of three-dimensional ellipsoid models.

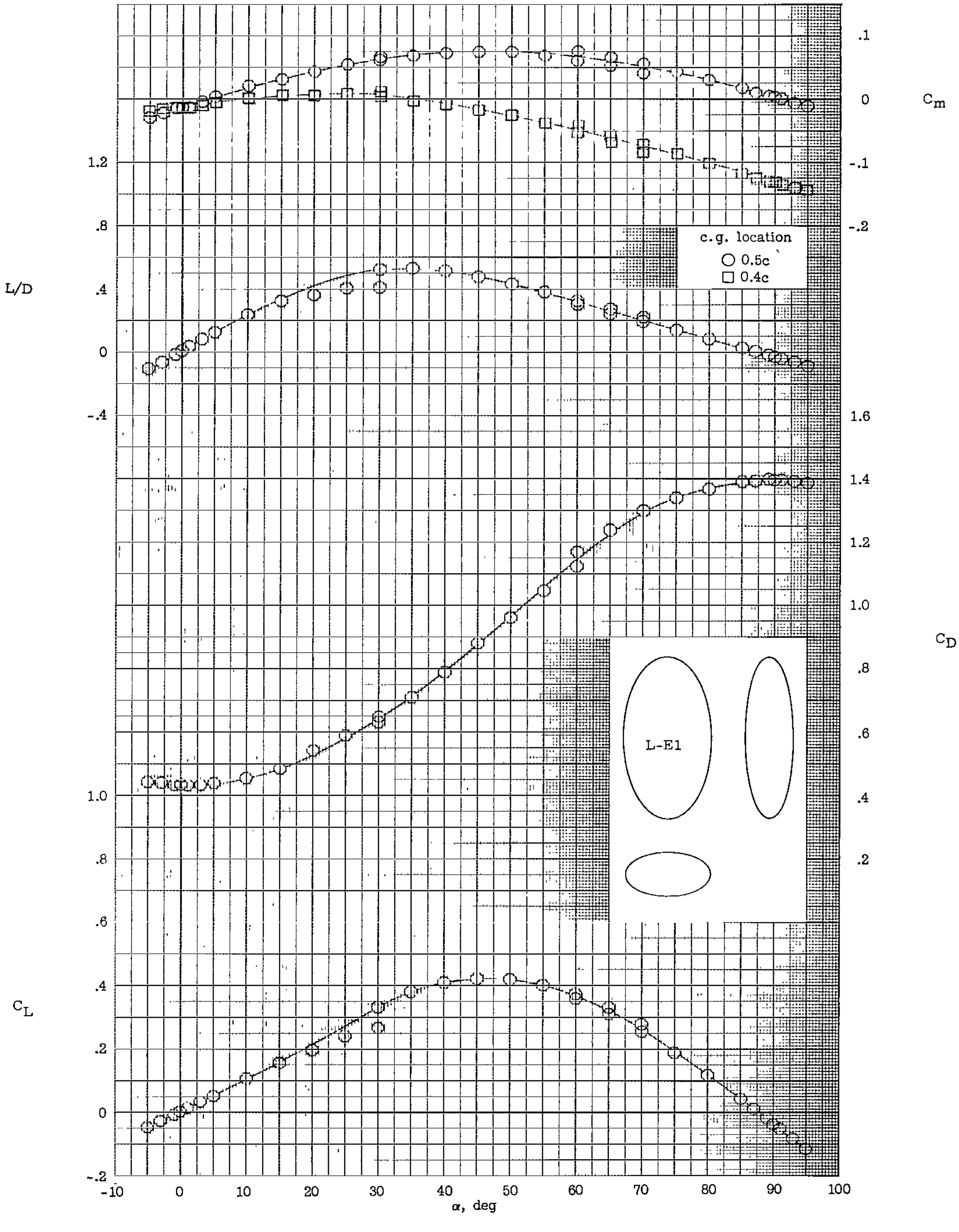

(b) L-E1 (t/c = 0.5).

Figure 5.- Continued.

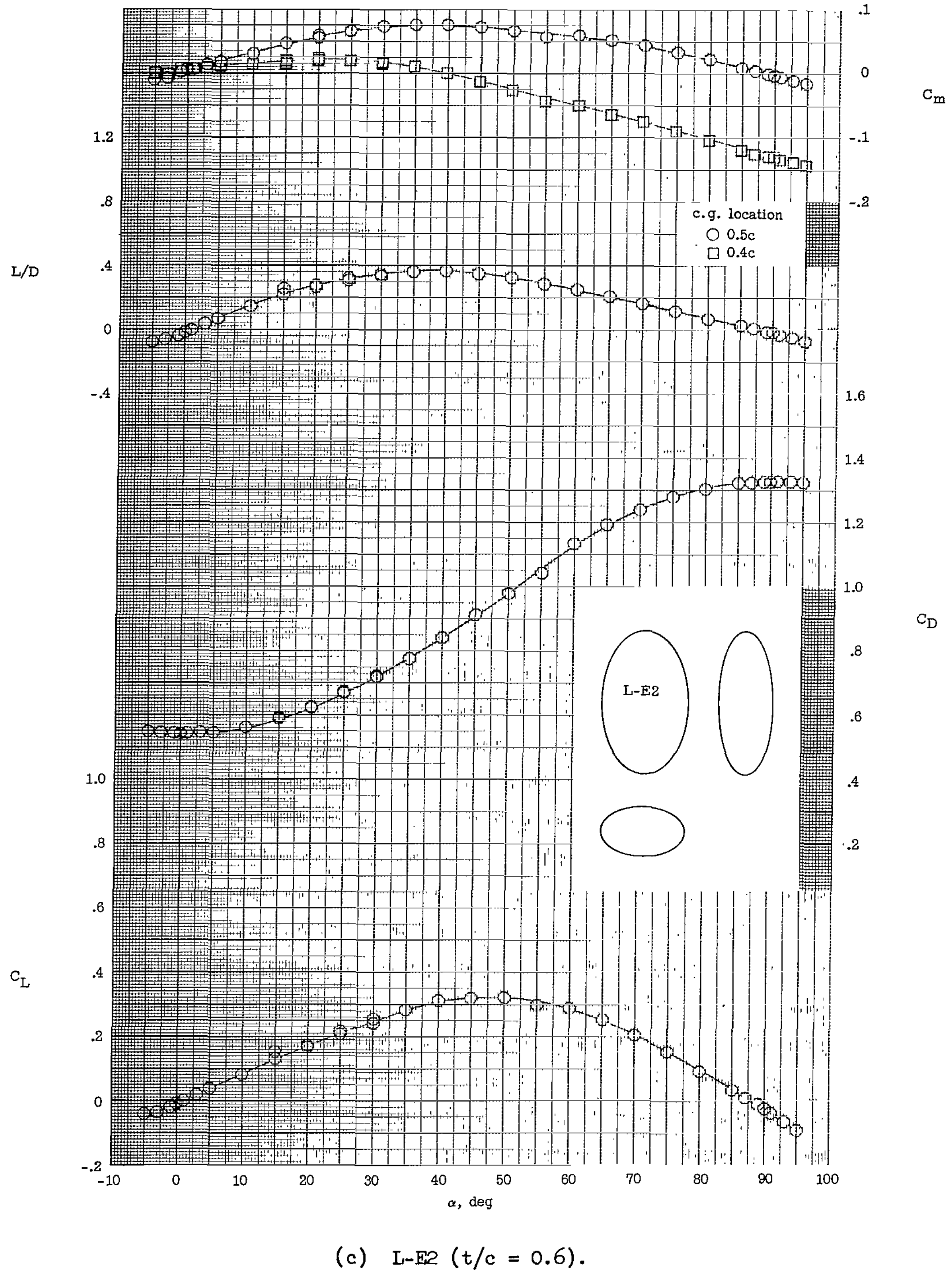

(c) L-E2 (t/c = 0.6).

Figure 5.- Continued.

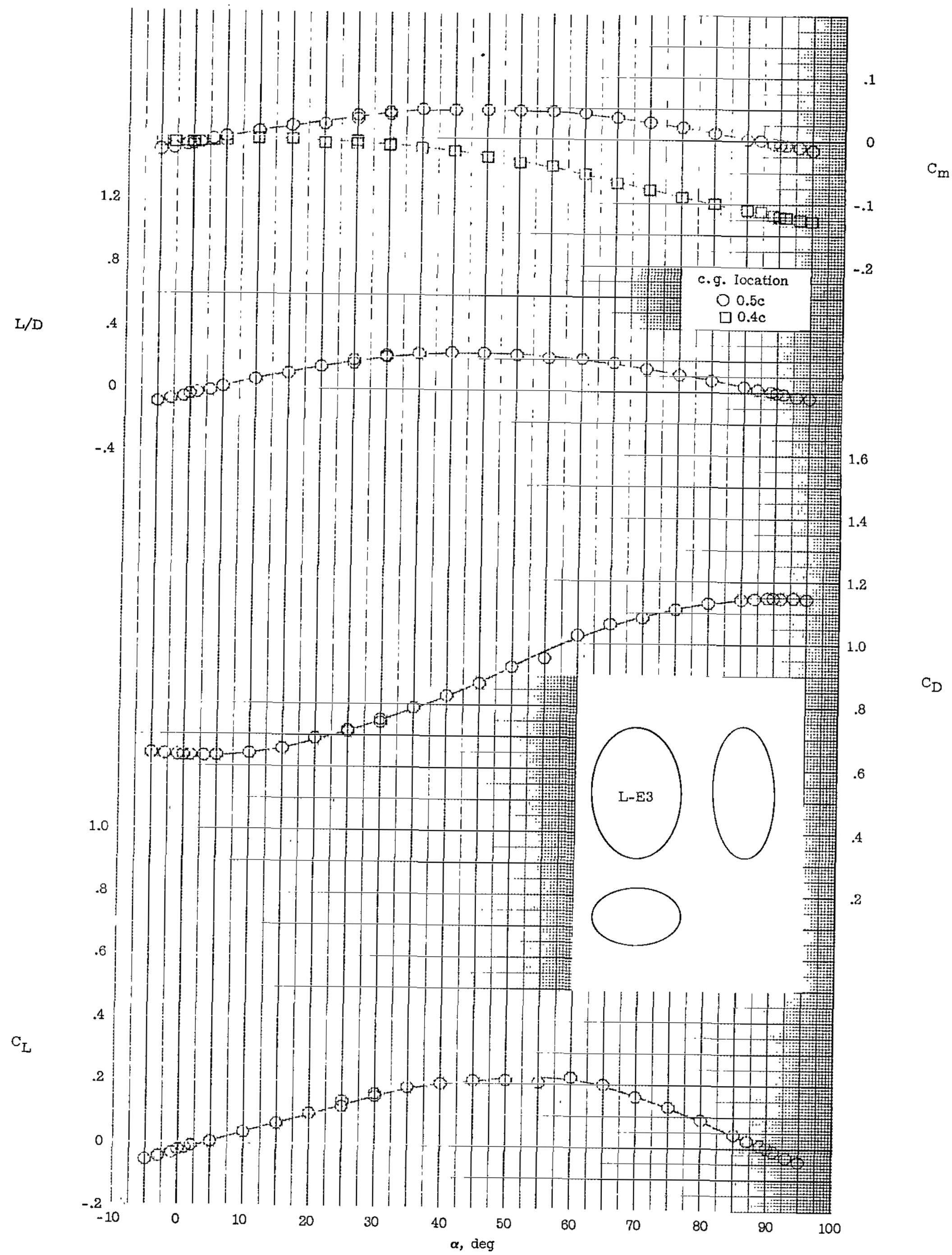

(d) L-E3 (t/c = 0.7).

Figure 5.- Continued.

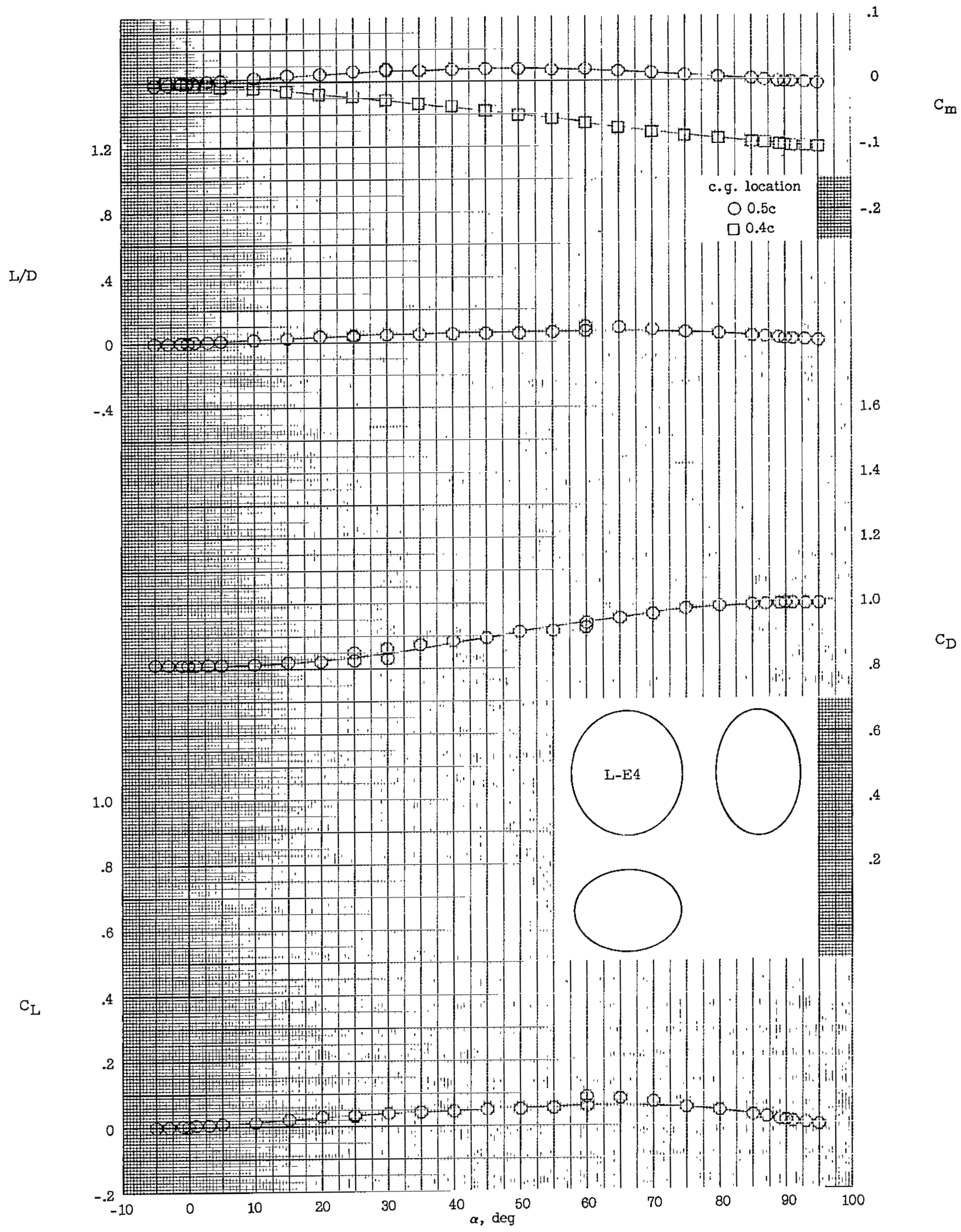

(e) L-E4 (t/c = 0.9).

Figure 5.- Concluded.

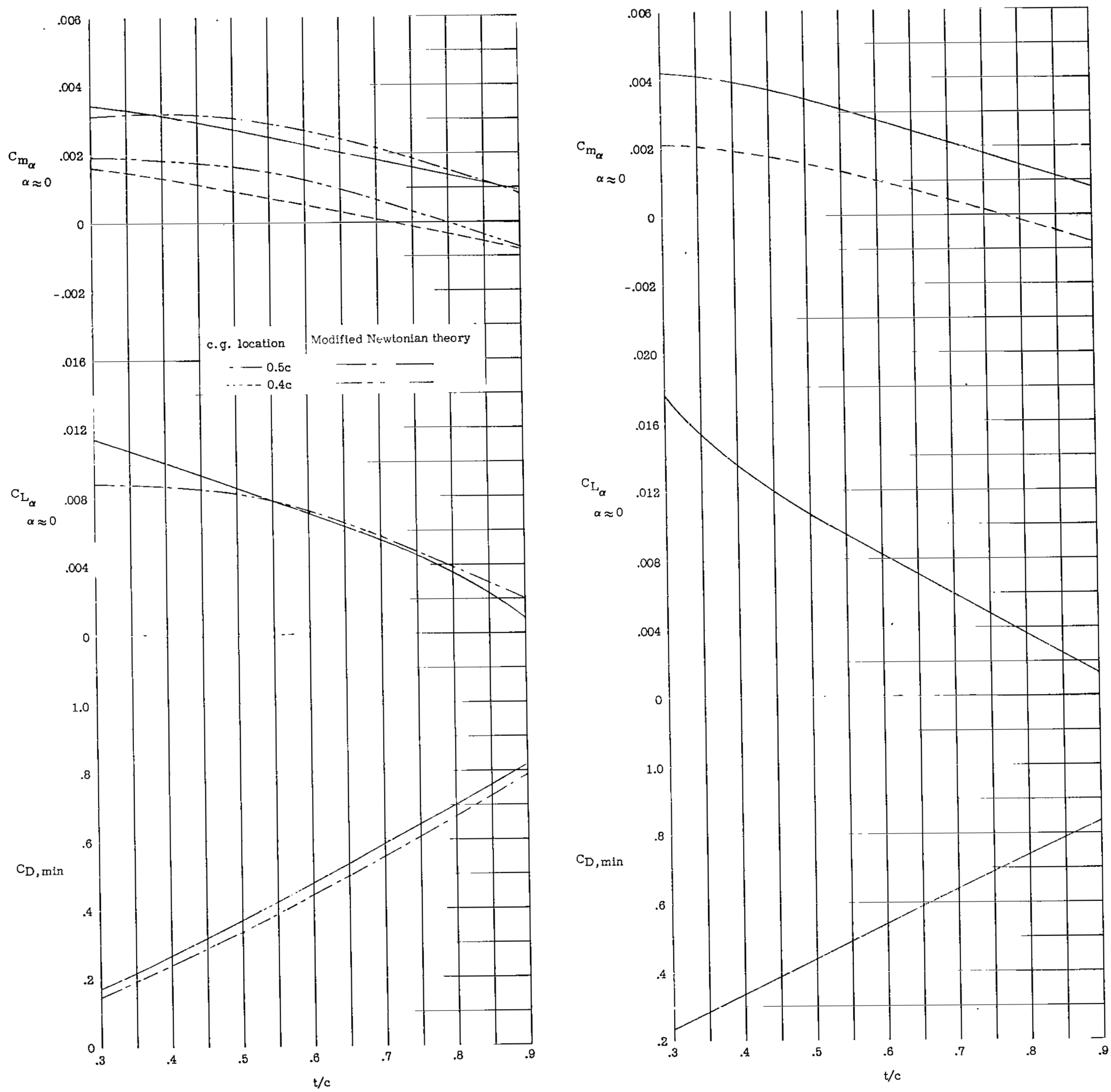

(a) Elliptic-lenticular models.

(b) Three-dimensional ellipsoid models.

Figure 6.- Summary of longitudinal aerodynamic parameters at low angles of attack for all model-thickness ratios.

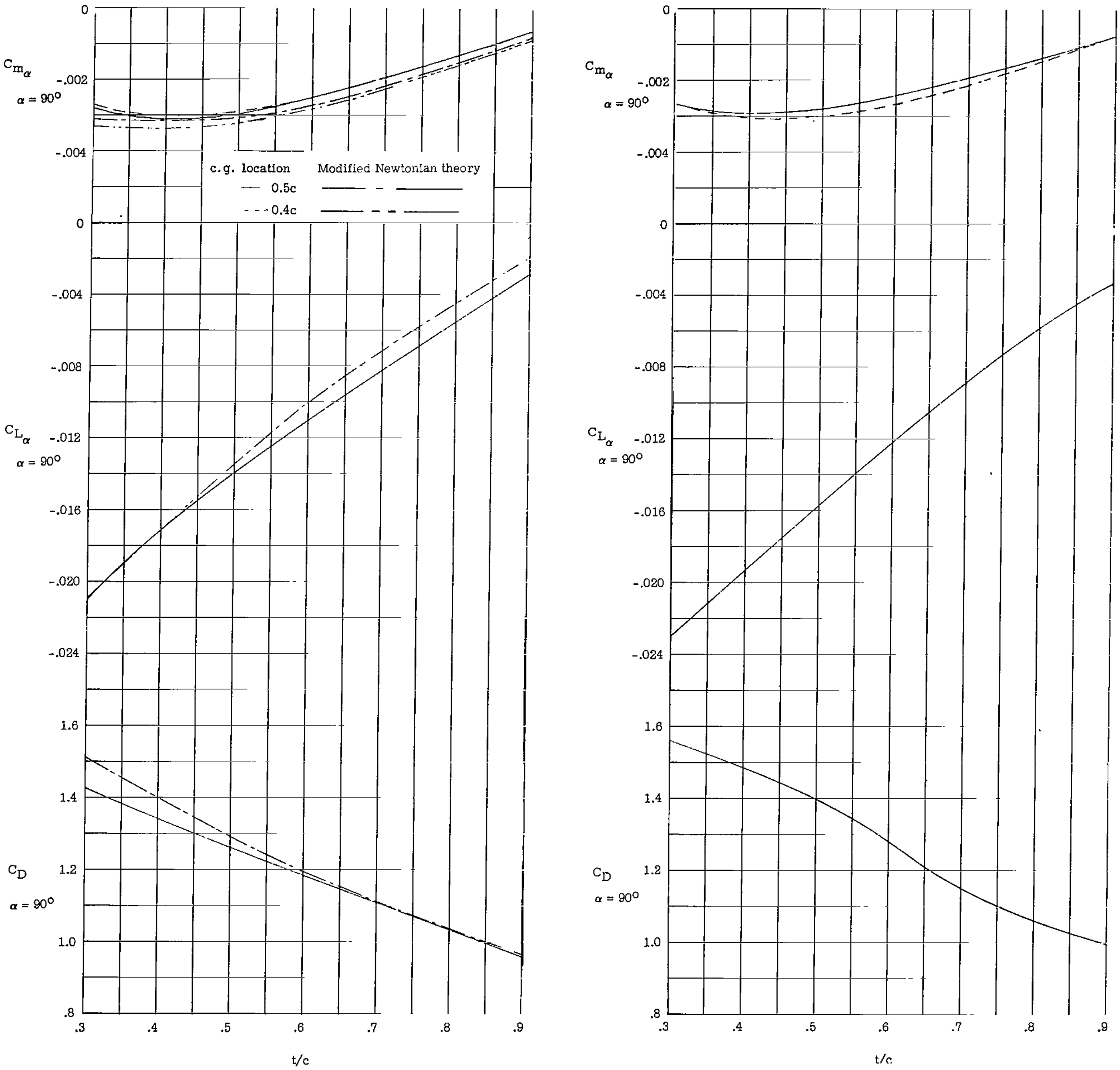

(a) Elliptic-lenticular models.

(b) Three-dimensional ellipsoid models.

Figure 7.- Summary of longitudinal aerodynamic parameters at an angle of attack of 90° for all model-thickness ratios.

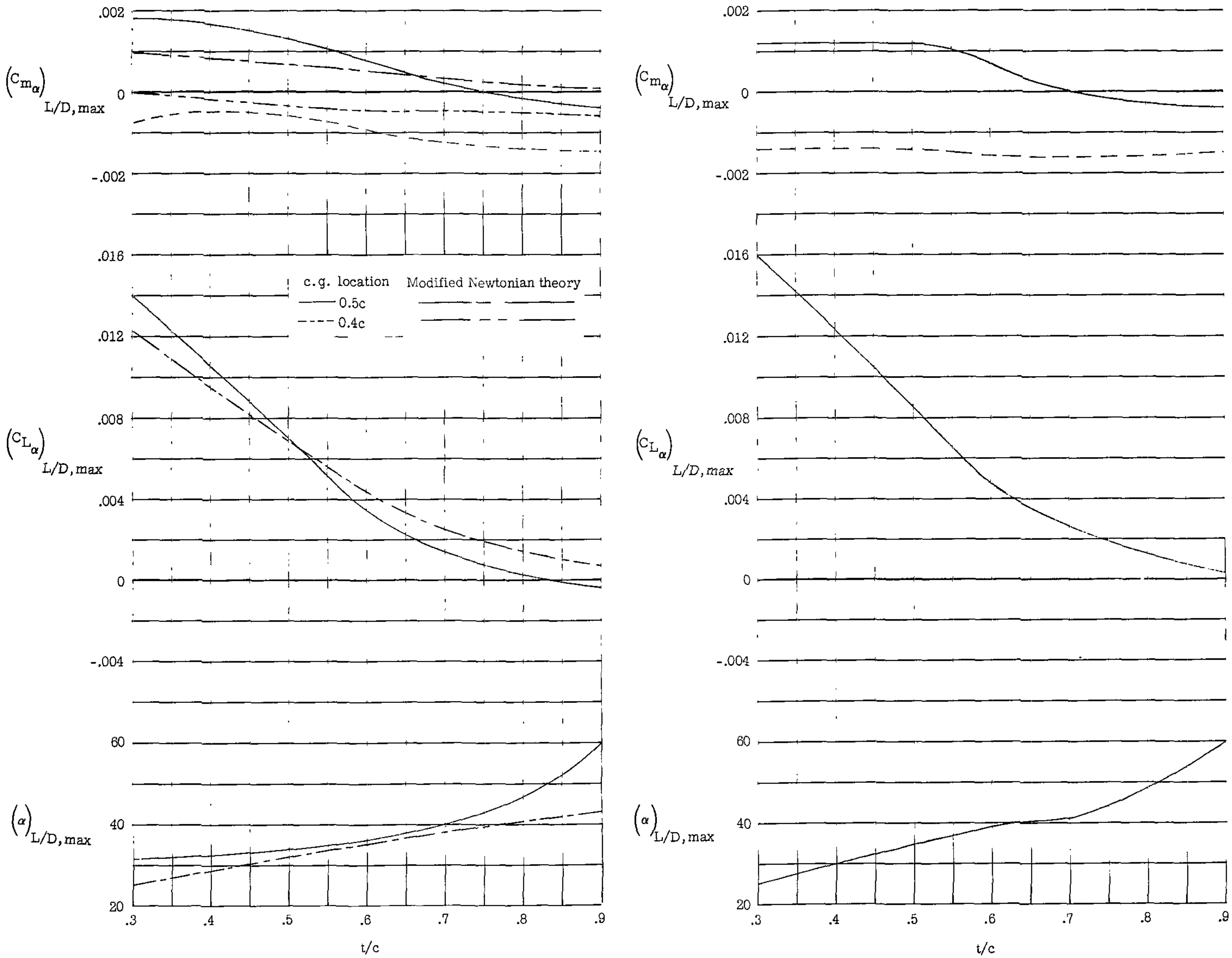

(a) Elliptic-lenticular models.

(b) Three-dimensional ellipsoid models.

Figure 8.- Summary of longitudinal aerodynamic parameters at maximum lift-drag ratio for all model-thickness ratios.

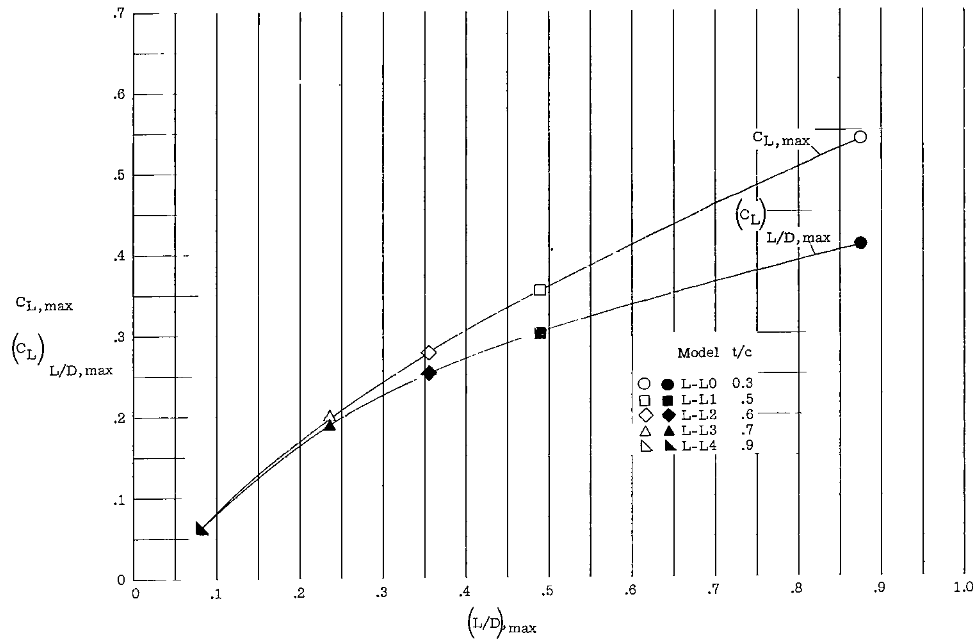

(a) Elliptic-lenticular models.

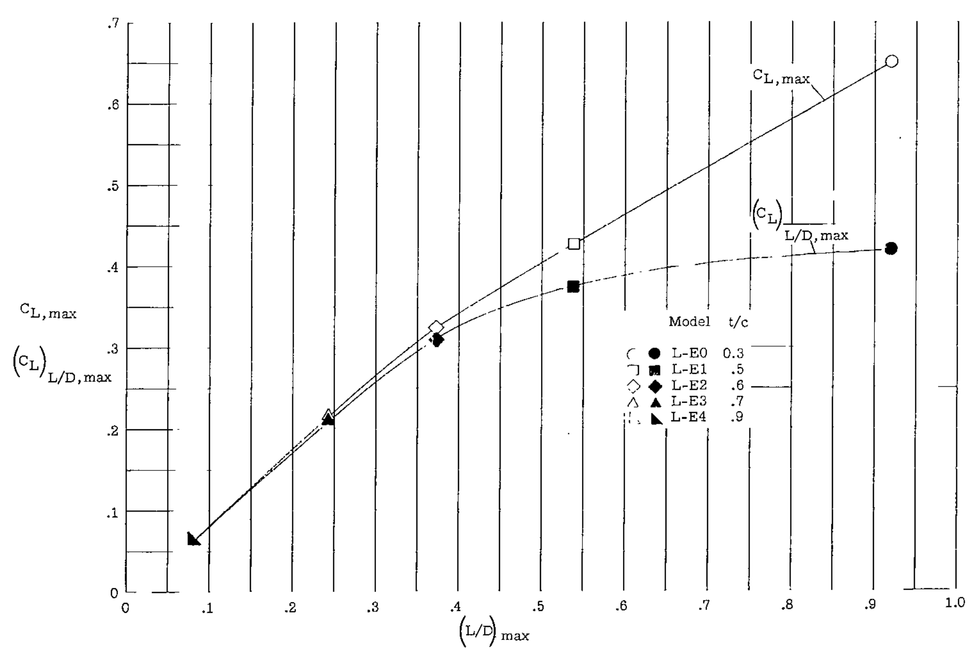

(b) Three-dimensional ellipsoid models.

Figure 9.- Comparison of lift coefficient at maximum lift-drag ratio with maximum lift coefficient for each model.

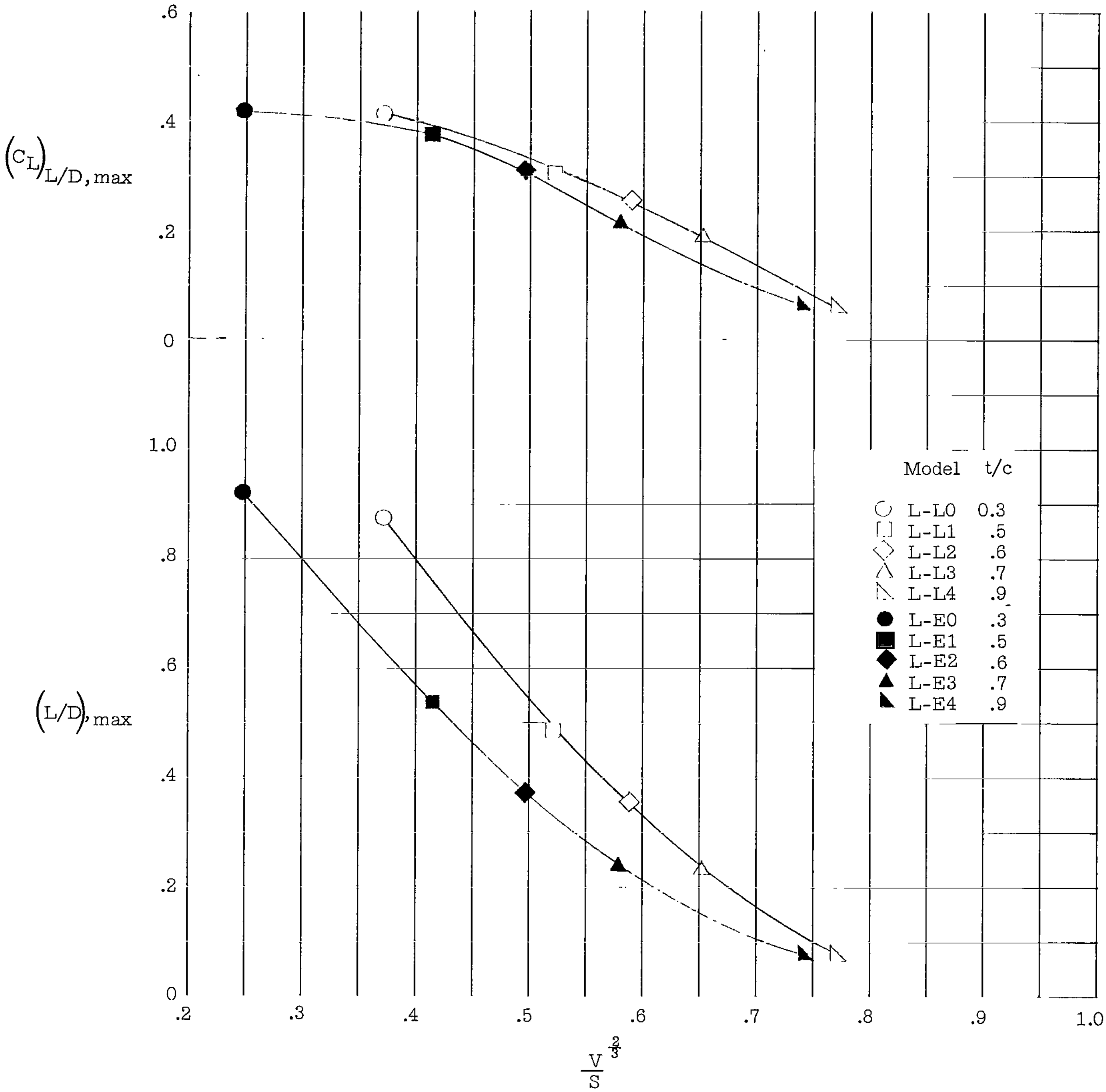

Figure 10.- Variation of maximum lift-drag ratio and lift coefficient at maximum lift-drag ratio with a volumetric efficiency parameter. Elliptic-lenticular models are shown as open symbols and three-dimensional ellipsoid models are shown as solid symbols.

"The aeronautical and space activities of the United States shall be conducted so as to contribute . . . to the expansion of human knowledge of phenomena in the atmosphere and space. The Administration shall provide for the widest practicable and appropriate dissemination of information concerning its activities and the results thereof."

—NATIONAL AERONAUTICS AND SPACE ACT OF 1958

NASA SCIENTIFIC AND TECHNICAL PUBLICATIONS

TECHNICAL REPORTS: Scientific and technical information considered important, complete, and a lasting contribution to existing knowledge.

TECHNICAL NOTES: Information less broad in scope but nevertheless of importance as a contribution to existing knowledge.

TECHNICAL MEMORANDUMS: Information receiving limited distribution because of preliminary data, security classification, or other reasons.

CONTRACTOR REPORTS: Technical information generated in connection with a NASA contract or grant and released under NASA auspices.

TECHNICAL TRANSLATIONS: Information published in a foreign language considered to merit NASA distribution in English.

TECHNICAL REPRINTS: Information derived from NASA activities and initially published in the form of journal articles.

SPECIAL PUBLICATIONS: Information derived from or of value to NASA activities but not necessarily reporting the results of individual NASA-programmed scientific efforts. Publications include conference proceedings, monographs, data compilations, handbooks, sourcebooks, and special bibliographies.

Details on the availability of these publications may be obtained from:

SCIENTIFIC AND TECHNICAL INFORMATION DIVISION

NATIONAL AERONAUTICS AND SPACE ADMINISTRATION

Washington, D.C. 20546